Materials Letters 224 (2018) 22–25

Contents lists available at ScienceDirect

Materials Letters

journal homepage: www.elsevier.com/locate/mlblue

Printability and microstructure of the CoCrFeMnNi high-entropy alloy fabricated by laser powder bed fusion

A. Piglione [a,*], B. Dovgyy [a], C. Liu [a], C.M. Gourlay [a], P.A. Hooper [b], M.S. Pham [a]

[a] Department of Materials, Imperial College London, Exhibition Road, London SW7 2AZ, UK
[b] Department of Mechanical Engineering, Imperial College London, Exhibition Road, London SW7 2AZ, UK

ARTICLE INFO

Article history:
Received 6 February 2018
Received in revised form 8 March 2018
Accepted 12 April 2018
Available online 12 April 2018

Keywords:
High-entropy alloys
Additive manufacturing
Laser powder bed fusion
Rapid cooling
Competitive growth
Epitaxial growth

ABSTRACT

The CoCrFeMnNi high-entropy alloy is a promising candidate for metal additive manufacturing. In this study, single-layer and multi-layer builds were produced by laser powder bed fusion to study microstructure formation in rapid cooling and its evolution during repeated metal deposition. CoCrFeMnNi showed good printability with high consolidation and uniform high hardness. It is shown that microstructure in the printed alloy is governed by epitaxial growth and competitive grain growth. As a consequence, a bi-directional scanning pattern without rotation in subsequent layers generates a dominant alternating sequence of two crystal orientations.
© 2018 The Authors. Published by Elsevier B.V. This is an open access article under the CC BY license (http://creativecommons.org/licenses/by/4.0/).

1. Introduction

High-entropy alloys (HEAs) are a unique class of alloys that contain five or more principal elements in near-equiatomic concentrations [1]. The equiatomic CoCrFeMnNi high-entropy alloy first introduced by Cantor et al. [2] exhibits a single-phase face-centred cubic (FCC) solid solution, and was selected for the current work as it possesses characteristics that are believed to make it particularly suitable for additive manufacturing (AM): (1) narrow freezing range [3], which minimises the risk of hot cracking; (2) outstanding oxidation resistance associated with a high concentration of Cr, which improves the consolidation of the builds; (3) FCC single-phase, which prevents inter-phase residual stresses originating from anisotropic thermal expansion/contraction during rapid cooling in AM. The current work assesses the printability of the CoCrFeMnNi alloy, which can be defined (following the definition of weldability proposed by David et al. [4]) as the ability of a material to be consolidated layer-upon-layer to form a designed part with desired microstructure and properties that ensure the performance of the printed material over its intended service life. In the current work, the alloy printability was evaluated by characterising its consolidation, solidification microstructure and hardness. Only two studies reported the AM fabrication of the CoCrFeMnNi HEA [5,6]; moreover, these studies did not provide in-depth investigations of solidification microstructures. Thus, the present work examined how microstructures form during rapid cooling and subsequently evolve following repeated deposition of metal. Such examination provides valuable insights into the relationship between print parameters and microstructure in AM builds.

2. Materials and methods

Pre-alloyed CoCrFeMnNi powder was provided by H.C. Starck Surface Technology & Ceramic Powders GmbH. The nominal composition can be found in Table 1. To understand how microstructures form during rapid solidification of the HEA, an eleven-track single-layer build was printed using a Renishaw AM250 on a 316L stainless steel substrate in argon atmosphere. A uni-directional scanning pattern was selected, with a power intensity of 200 W, a hatch spacing of 125 μm, an exposure time of 80 μs and a point distance of 60 μm. To understand crystal growth in a multi-layer build, a $10 \times 10 \times 10$ mm cubic build was printed using a bi-directional pattern without rotation of the scan pattern along the build direction. It was printed with the same parameters described above except for a reduced hatch spacing of 85 μm, to increase the consolidation of the build. X-ray diffraction (XRD) was performed using a Bruker D2 Phaser. Density measurements of the cubic build were carried out both by using Archimedes'

* Corresponding author.
E-mail address: alessandro.piglione16@imperial.ac.uk (A. Piglione).

https://doi.org/10.1016/j.matlet.2018.04.052
0167-577X/© 2018 The Authors. Published by Elsevier B.V.
This is an open access article under the CC BY license (http://creativecommons.org/licenses/by/4.0/).

Table 1
Nominal composition of the HEA powder.

Element	Co	Cr	Fe	Mn	Ni
wt%	Balance	18.2	19.5	17.9	21.2

principle and by measuring its consolidated fraction in optical micrographs. Sequences of Vickers hardness tests were carried out applying a 1 kg load for 10 s. Energy-dispersive X-ray spectroscopy (EDX) was carried out on a polished surface of the cubic build using a JEOL 6010LA scanning electron microscope (SEM). Polished samples were then electrochemically etched in a 10% oxalic acid solution for 90 s at 2.50 V. Subsequently, SEM imaging and electron backscatter diffraction (EBSD) were carried out on etched samples using a Zeiss Auriga.

3. Results and discussion

3.1. XRD, EDX, density measurements and hardness

Fig. 1a shows XRD profiles of the as-received powder and of the cubic build. Only a single FCC phase was detected, showing that the near-equiatomic combination of these five elements leads to a single phase in additive manufacturing, in good agreement with previous studies [5,6]. The strong intensity of the (2 0 0) peak in the XRD profile of the cubic build indicates a preferred ⟨0 0 1⟩ grain orientation, in contrast with rather randomly oriented grains in the powder.

The measurement of the density of the cubic build yielded a relative density of 99.29% using Archimedes' principle and 99.88% by analysing micrographs. The hardness test results are shown in Fig. 1b. These results show that there is no significant variation in hardness along the build direction in two different regions of the build. The average measured hardness was of 212 HV1, which is significantly higher with respect to those previously reported for the CoCrFeMnNi alloy [5,6]. The measured high relative density, coupled with high and homogeneous hardness, indicates an excellent consolidation of the fabricated HEA.

EDX mapping (Fig. 1c) was carried out in a region that includes the interface between the substrate and the CoCrFeMnNi build, which can be clearly seen thanks to the contrast originating from the differences in element concentrations. Transients of element concentrations due to mixing between the two materials can be observed in the first layers of the cubic build. A homogeneous

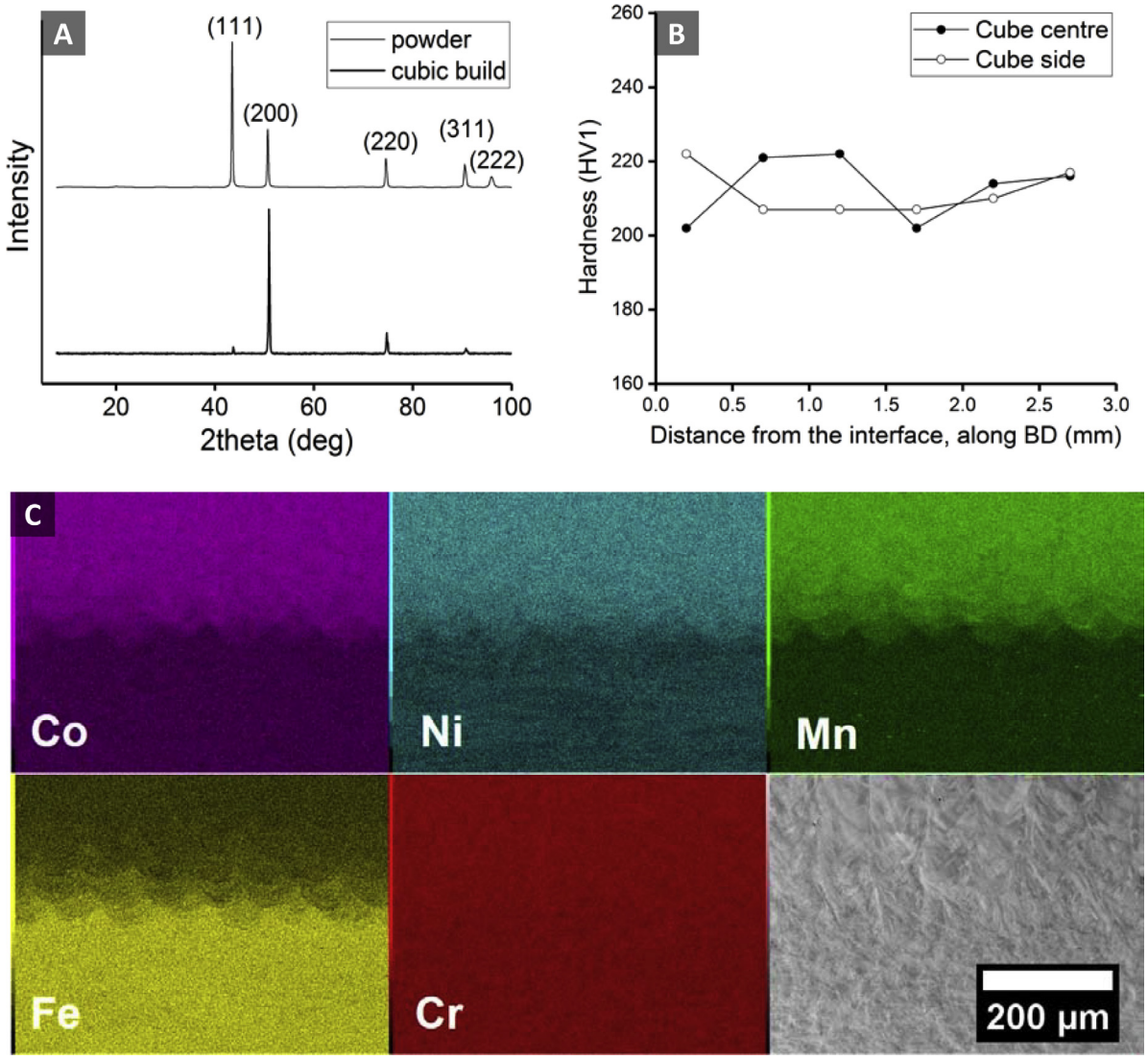

Fig. 1. (a) XRD profiles of the HEA powder and the cubic build, (b) hardness measurements along the build direction and (c) elemental maps for the elements of the HEA in a region at the interface between the substrate and the HEA build.

composition distribution is found in the bulk of the HEA cube, with no evidence of elemental segregation at the lengthscale of Fig. 1c.

3.2. Solidification microstructure

Fig. 2 shows a SEM micrograph (a) and the related EBSD IPF-y map (b) of a cross-section of one track in the single-layer build. Local melting on a cold substrate induced a high cooling rate, resulting in very fine cells within the melt-pool (Fig. 2c and d). The cell spacings were found to range from 0.52 μm to 0.64 μm, with an average of 0.59 μm. These solidification cells are much finer compared to those reported by previous studies of the same alloy [5], thus explaining the high hardness values showed in Section 3.1: since cell boundaries can restrict dislocation movement during plastic deformation, the presence of finer cells increases macroscopic hardness [7]. Heat conduction through the substrate is the dominant heat transfer mechanism in LPBF. In addition, the heat flux is highest at the solid-liquid interface. Thus, the direction perpendicular to the melt-pool profile (i.e., fusion line) is the direction of maximum heat flux in regions near the fusion line. Fig. 2a shows multiple cell domains growing epitaxially from existing grains in the substrate, with their cell axis perpendicular to the fusion line. Furthermore, the EBSD scan of Fig. 2b shows that cells are oriented with one of their ⟨0 0 1⟩ orientations normal to the fusion line. In other words, cells are found to have both their cell axis and one ⟨0 0 1⟩ orientation (i.e., the preferred growth direction in FCC crystals) aligned with the direction of maximum heat flux. This is in good agreement with previous studies on solidification [8]. The alignment of the preferred growth direction and the thermal gradient is then found to be responsible for the survival of some grains (i.e., cell domains with the same crystallographic orientation) over others during solidification. When neighbouring grains impinged upon each other, they competed for growth: the grain whose preferred growth direction was better aligned with the direction of maximum heat flux in that region survived and outgrew others which were misaligned with the thermal gradient [3]. As an example, grain g1 outgrew grain g2 in the central region of the melt-pool (Fig. 2b).

The grain structure of an analogous region in the multi-layer cubic build is significantly different to that of the single-layer build. Fig. 3b and c show the microstructures in two adjacent tracks at the substrate/HEA interface. In each melt-pool, fine cells grew epitaxially from existing grains in the substrate, similar to what was observed in the single-layer build, or equivalently from existing cells in underlying deposited layers. However, the number of grains in the cubic build is substantially reduced because each melt-pool underwent multiple remelting events due to the deposition of adjacent tracks and successive layers, promoting grain selection via growth competition: favourably aligned grains outgrew misaligned ones, resulting in the reduction in number of grains as the print progressed. This becomes evident in the bulk of the cubic build (Fig. 3a). Since there was no rotation between the N and the N + 1 layer, melt-pools were stacked in columns along the build direction (BD). Thus, the thermal profile of each melt-pool was repeated in the melt-pool of the layer above it, resulting in a global thermal gradient along BD and hence providing preferred conditions for columnar growth. This scanning pattern, coupled with epitaxial growth and grain selection after remelting, led to the presence of an alternating sequence of columnar grains with only two dominant crystallographic orientations (Fig. 3a). Red grains (with one ⟨0 0 1⟩ orientation parallel to BD) are confined to narrow regions at the centre of each melt-pool column, whilst green grains (with one ⟨0 1 1⟩ orientation parallel to BD) are wider and extend across the sides of two adjacent melt-pools, with the ⟨0 0 1⟩ orientation inclined at 45° with respect to BD. In both cases the preferred growth direction is aligned with the direction of maximum heat flux in that region, thus confirming the grain selection mechanisms described above. Fig. 3a also shows

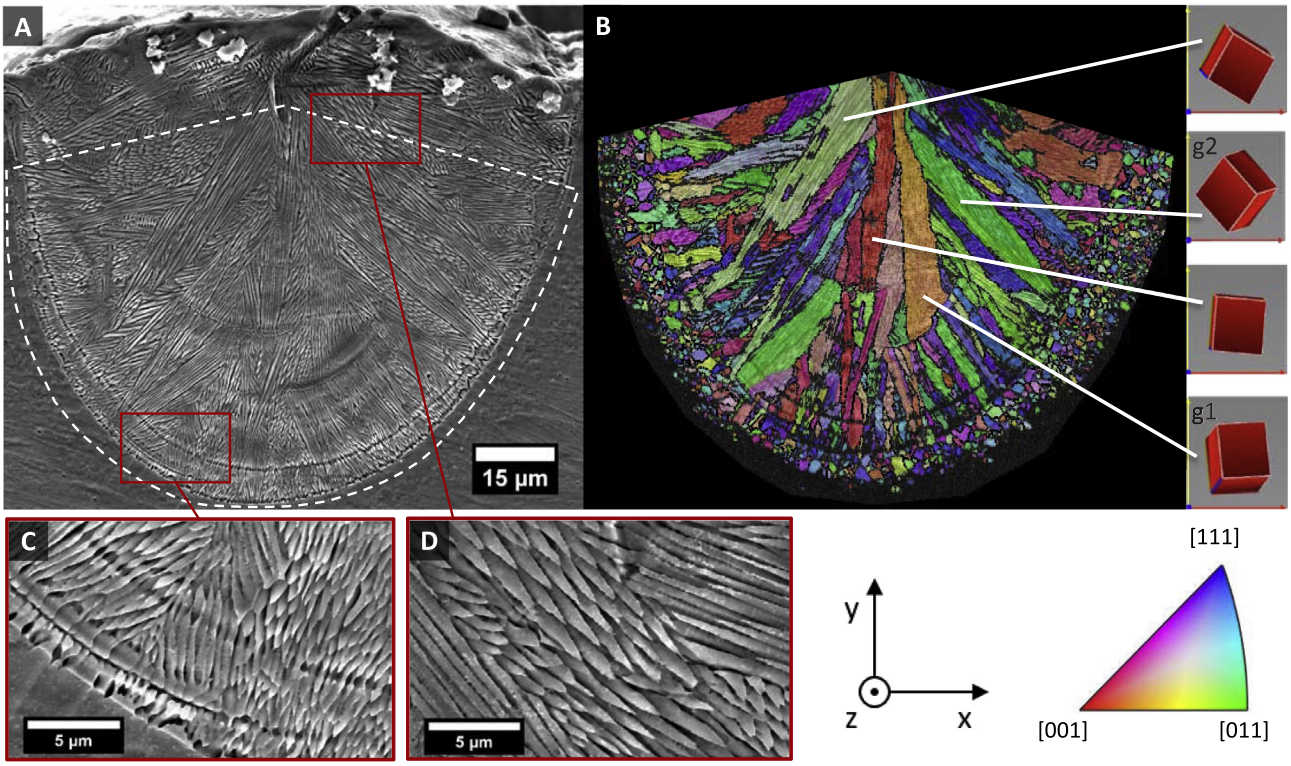

Fig. 2. SEM micrograph (a) and related EBSD IPF-y map (b) of the cross-section of one track. The cubes surrounding the EBSD map show the crystallographic orientations of selected grains. SEM micrographs (c and d) show the cellular structure in greater detail.

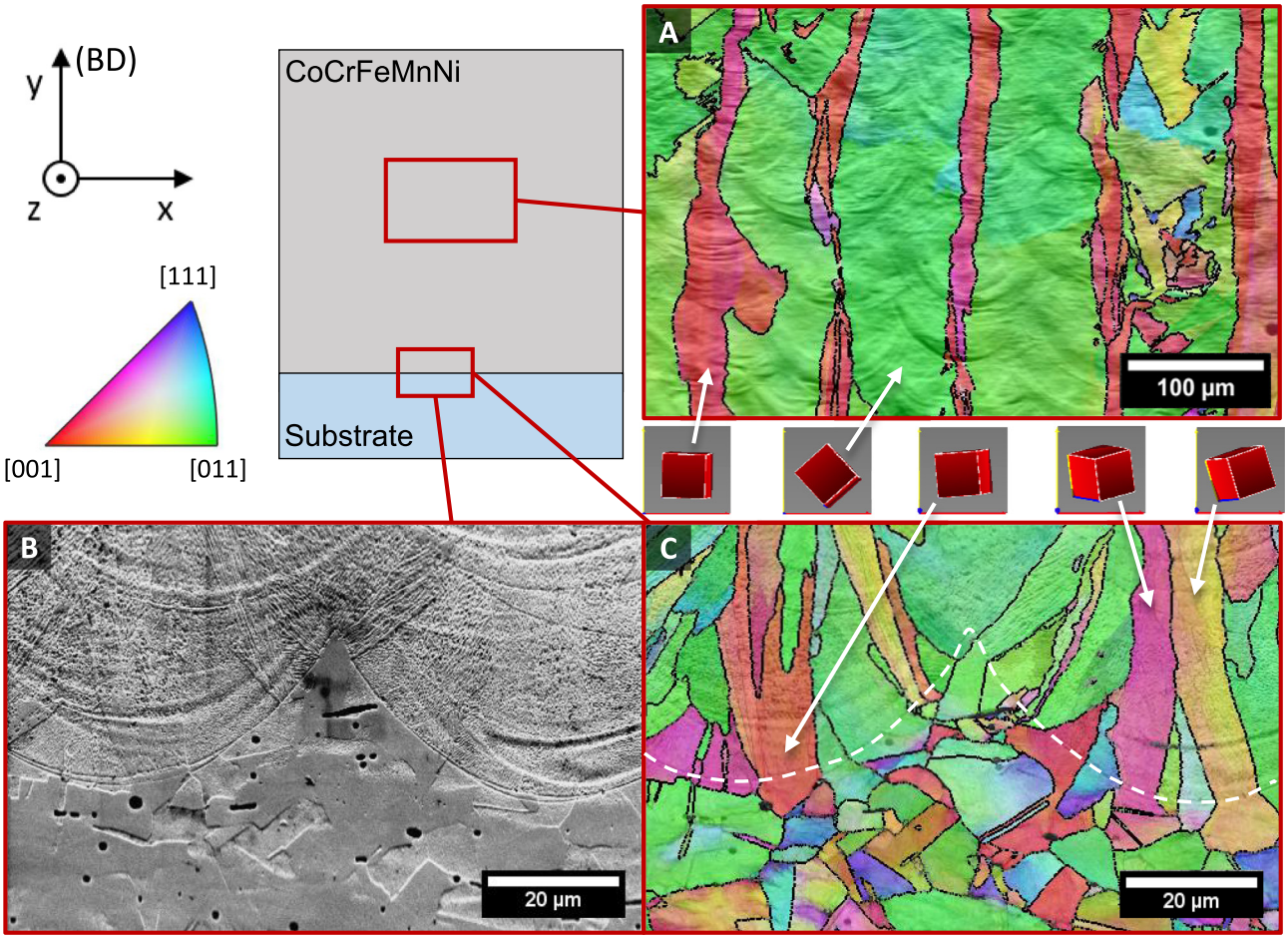

Fig. 3. EBSD IPF-y map of a region in the cubic build (a); SEM micrograph and related EBSD IPF-y map of a region at the substrate/build interface (b and c).

some grain boundaries which appear straight and partly consist of coincident site lattices (e.g. Σ3 and Σ5). Considering that boundaries with small Σ numbers typically have special properties [9], it would be interesting to study the characteristics of boundaries in the printed alloy in the future.

4. Conclusions

The CoCrFeMnNi high-entropy alloy exhibits very good printability by laser powder bed fusion: it has a FCC single-phase coupled with a high degree of consolidation, and good hardness without macrosegregation. Studies of microstructures have shown that, whilst rapid cooling of molten metal on existing grains leads to the epitaxial growth of fine cells in melt-pools, the remelting induced by the repeated deposition of metal leads to grain selection via competitive growth. The choice of a bi-directional scanning pattern without rotation promotes the growth of columnar grains, which form an alternating sequence of two dominant crystallographic orientations.

Acknowledgements

This work was supported by EPSRC (Grant EP/K503733/1) and AWE Plc.

References

[1] E.J. Pickering, N.G. Jones, Int. Mater. Rev. 61 (2016) 183–202.
[2] B. Cantor, I.T.H. Chang, P. Knight, A.J.B. Vincent, Mater. Sci. Eng. A 375 (2004) 213–218.
[3] Z. Wu, S.A. David, Z. Feng, H. Bei, Scr. Mater. 124 (2016) 81–85.
[4] S.A. David, J.A. Siefert, Z. Feng, Sci. Technol. Weld. Join. 18 (2013) 631–651.
[5] C. Haase, F. Tang, M.B. Wilms, A. Weisheit, B. Hallstedt, Mater. Sci. Eng. A 688 (2017) 180–189.
[6] N. Eißmann, B. Klöden, T. Weißgärber, B. Kieback, Powder Metall. 5899 (2017) 1–14.
[7] M.S. Pham, B. Dovgyy, P.A. Hooper, Mater. Sci. Eng. A 704 (2017) 102–111.
[8] W.J. Boettinger, S.R. Coriell, A.L. Greer, A. Karma, W. Kurz, M. Rappaz, R. Trivedi, Acta Mater. 48 (2000) 43–70.
[9] B.B. Straumal, O.A. Kogtenkova, A.S. Gornakova, V.G. Sursaeva, B. Baretzky, J. Mater. Sci. 51 (2015) 382–404.